Kinetic Stabilization of Microtubule Dynamics at Steady State by Tau and Microtubule-Binding Domains of Tau[†]

Dulal Panda,[‡] Bruce L. Goode,[§] Stuart C. Feinstein,[§] and Leslie Wilson*,[‡]

Division of Molecular, Cellular, and Developmental Biology, Department of Biological Sciences, and The Neuroscience Research Institute, University of California, Santa Barbara, California 93106

Received March 23, 1995; Revised Manuscript Received June 15, 1995[⊗]

ABSTRACT: Tau is a neuronal microtubule-associated protein that plays an important role in stabilizing axonal microtubules and maintaining neuronal processes. To investigate the mechanisms by which tau performs these functions, we have determined the actions of full-length adult tau and tau peptides corresponding to two different microtubule-binding domains of tau (the first repeat, R1, VRSKIGSTENLKHQPGGG, and the first interrepeat, R1-R2 IR, KVQIINKK) on the growing and shortening dynamics at the plus ends of individual microtubules at steady state. Tau suppressed steady-state microtubule dynamics at very low molar ratios of tau to tubulin. At the lowest ratios examined (tau:tubulin ratios of 1:175 and 1:85), suppression of dynamics occurred in the absence of a detectable change in polymer mass. Tau reduced the mean rate and extent of shortening *and*, in contrast to previous work carried out under conditions of net polymer gain, tau also suppressed the mean rate and extent of growing. Tau also strongly increased the rescue frequency, it moderately suppressed the catastrophe frequency and it strongly increased the percentage of total time that the microtubules spent in an attenuated (pause) state, neither growing nor shortening detectably. In addition, both the R1 and R1-R2 IR tau peptides suppressed steady-state microtubule dynamics in a sequence-specific manner and in a manner that was qualitatively indistinguishable from full-length tau. The data provide significant support for a mechanism in which the binding of tau to individual tubulin subunits in microtubules induces a conformational change that strengthens inter-tubulin bonding.

Microtubules, 25 nm diameter tube-shaped polymers composed of the $\alpha\beta$ heterodimeric protein tubulin, play important roles in many cellular processes such as mitosis, the trafficking of intracellular vesicles, and the formation and function of axons and dendrites of neurons [reviewed in Dustin (1984); Diaz-Nido et al., 1990]. Microtubules are intrinsically dynamic polymers, and there is considerable evidence that their dynamic properties, which are critically involved in many of their functions, are finely regulated [reviewed by McIntosh (1994); Wordeman & Mitchison, 1994; Desai & Mitchison, 1995]. In axons, for example, large numbers of microtubules are arranged into an elaborate and relatively stable network that functions as a cytoskeletal support for the axon and for the transport of materials between the neuronal cell body and the tip of the axon. In contrast, microtubules in the growth cone of developing axons are highly dynamic and appear to be important in promoting growth cone movement and in establishing interneuronal connections (Tanaka & Kirschner, 1991; Tanaka et al., 1995). The stability of axonal microtubules is thought to be controlled in large part by the binding of microtubule-associated proteins (MAPs)[1] along their surfaces (Horio & Hotani, 1986; Farrell et al., 1987; Pryer et al., 1992; Drechsel et al., 1992; Kowalski & Williams, 1993; Toso et al., 1993).

Microtubules exhibit at least two types of unusual non-equilibrium dynamics. Both *in vitro* and in cells, microtubule ends switch between growing and shortening states, a behavior termed "dynamic instability" (Mitchison & Kirschner, 1984; Horio & Hotani, 1986; Walker et al., 1988), due to the gain and loss of a stabilizing cap at the microtubule ends thought to consist of tubulin-liganded GTP or GDP·P_i (Carlier, 1989; Erickson & O'Brien, 1992). Also *in vitro* and in cells at polymer mass steady state net growth of microtubules in a population can occur at one microtubule end and net shortening can occur at the opposite end, a behavior termed "treadmilling" or "flux" (Margolis & Wilson, 1978; Hotani & Horio, 1987; Farrell et al., 1987; Mitchison, 1989; Sawin & Mitchison, 1991). Both dynamic behaviors are strongly modulated by MAPs *in vitro* (Horio & Hotani, 1986; Farrell et al., 1987; Pryer et al., 1992; Drechsel et al., 1992; Kowalski & Williams, 1993; Toso et al., 1993; Yamauchi et al., 1993), suggesting that MAPs may influence microtubule dynamics in a similar fashion in living cells.

One prominent MAP that appears to be important in modulating microtubule dynamics in axons is tau. Tau is a family of developmentally regulated phosphoproteins expressed primarily in neurons and localized to axons [for reviews see Diaz-Nido et al. (1990), Wiche et al. (1991), and Goedert et al. (1994)]. Tau was first identified by its

[†] This work was supported by USPHS Grant NS13560 from the National Institute of Neurological Diseases and Stroke (L.W. and D.P.) and by Grant 93-18637 from the California Department of Health (Alzheimer's Disease Program; S.C.F. and B.L.G.).

[‡] Department of Biological Sciences.

[§] The Neuroscience Research Institute.

[⊗] Abstract published in *Advance ACS Abstracts,* August 15, 1995.

[1] Abbreviations: EGTA, ethylenebis(oxyethylenenitrilo)tetraacetic acid; GDP, guanosine 5′-diphosphate; GTP, guanosine 5′-triphosphate; Mes, 2-morpholinoethanesulfonic acid; Pipes, 1,4-piperazinediethanesulfonic acid; IR, interrepeat; MAPs, microtubule-associated proteins; PME buffer, 50 mM Pipes, 1 mM EGTA, and 1 mM $MgCl_2$, pH 6.8; PMME buffer, 87 mM Pipes, 36 mM Mes, 1.4 mM $MgCl_2$, and 1 mM EDTA, pH 6.8.

0006-2960/95/0434-11117$09.00/0

ability to copolymerize with tubulin and promote microtubule nucleation and elongation (Weingarten et al., 1975; Cleveland et al., 1977a). In neurons, tau colocalizes with axonal microtubules (Binder et al., 1985; Drubin et al., 1986; Kosik & Finch, 1987), it promotes microtubule formation (Drubin & Kirschner, 1986), and it stabilizes microtubules when microinjected in non-neuronal cells (Drubin et al., 1986). Expression of tau has been shown to coincide with the extension of neurites during cell differentiation (Binder et al., 1985; Drubin et al., 1985; Kosik & Finch, 1987), and antisense studies indicate that tau has a role in the development and maintenance of the axon-like process of PC-12 cells (Esmaeli-Azad et al., 1994) and in the establishment of neuritic polarity in primary cerebellar neurons (Caceres & Kosik, 1990; Kosik & Caceres, 1991). Tau is also the primary component of one of the pathological hallmarks of Alzheimer's disease, the paired helical filaments [reviewed in Goedert et al. (1994); Goedert et al., 1989a; Grundke-Iqbal et al., 1986]. In Alzheimer's disease, tau has lost its affinity for microtubules and is assembled into the paired helical filaments and neurofibrillary tangles, a process that may lead to neuronal degeneration.

Tau isolated from adult brain is a mixture of six related isoforms having an apparent molecular mass of 40−58 kDa. The basis of the heterogeneity appears to be a combination of alternate mRNA splicing (Goedert et al., 1989a,b; Himmler et al., 1989; Himmler, 1989; Kosik et al., 1989) and differential phosphorylation (Butler & Shelanski, 1986). Tau contains a highly basic C-terminal microtubule-binding domain and an N-terminal projection domain (Hirokawa et al., 1988; Lee et al., 1988, 1989; Goedert et al., 1989a,b; Himmler et al., 1989; Himmler, 1989). The microtubule-binding domain consists of either three or four tandemly repeated 18-amino acid residues, which are separated by 13−14-amino acid interrepeat (IR) regions. In addition, the proline-rich middle region of tau located amino terminal to the repeat region has been reported to contain significant microtubule binding activity (Butner & Kirschner, 1991; Brandt & Lee, 1993; Goode & Feinstein, 1994; Gustke et al., 1994). An *in vitro*-translated tau peptide consisting of the first tubulin-binding repeat is able to bind to microtubules *in vitro*, and an increase in the number of repeats increases the efficiency of microtubule binding (Butner & Kirschner, 1991). In addition, a synthetic peptide consisting of the first 18-amino acid tau repeat can stimulate the assembly of purified tubulin into microtubules (Ennulat et al., 1989; Maccioni et al., 1989). However, the molar concentration of peptide required to promote polymerization is very high compared to the concentration required for native tau, indicating that the repeat peptides are less potent than the full-length protein. Recently, Goode and Feinstein (1994) found that the IR region between repeat 1 (R1) and repeat 2 (R2) can also bind to microtubules and that a synthetic peptide corresponding to just 10 amino acids of the R1-R2 interrepeat is sufficient to promote tubulin polymerization. From a developmental point of view, it is especially notable that the R1-R2 IR domain is expressed solely in adult, but not fetal, isoforms of tau.

Previous studies on the action of tau on microtubule polymerization in bulk solution or on the growing and shortening dynamics of individual microtubules have been carried out under conditions of net polymer gain. In these studies, tau has been found to stimulate microtubule nucleation, reduce the subunit critical concentration, increase the rate of microtubule elongation, and decrease the transition frequency from growing to shortening (Weingarten et al., 1975; Cleveland et al., 1977a; Bré & Karsenti, 1990; Drechsel et al., 1992; Pryer et al., 1992). Such conditions may exist in cells, for example, during neuronal process outgrowth when microtubule polymer mass is increasing rapidly (Drubin et al., 1985). However, once formed, neuronal processes become relatively stable and do not undergo dramatic length changes. In mature neurons, it is reasonable to suspect that the mass of microtubule polymer does not change appreciably and that microtubule functions that involve the dynamics of microtubules occur at or near polymer mass steady state. While axonal microtubules exhibit some dynamic behavior, they are relatively stable in general (Bamburg et al., 1986; Donoso, 1986; Okabe & Hirokawa, 1988, 1990) compared with mitotic spindle microtubules, many microtubules found in the interphase cytoskeleton, or microtubules in the growth cone of growing axons. The stability and structural integrity of axonal microtubules are likely to be important in their function as evidenced by pharmacological studies (Yamada et al., 1971; Drubin et al., 1986; Diaz-Nido et al., 1990; Baas & Black, 1990; Baas et al., 1994). Thus, in order to understand tau action in a mature neuron, it is important to investigate the effects of tau on microtubule dynamics at steady state.

In this report, we have analyzed the actions of full-length adult tau at low molar ratios of tau to tubulin on polymerization dynamics at the plus ends of bovine brain microtubules at polymer mass steady state by differential interference contrast video microscopy. We used ratios of tau to tubulin that span the range found in undifferentiated and differentiated neuronal (PC-12) cells (Drubin et al., 1985). We also compared the effects on microtubule dynamics of full-length tau to the effects of synthetic peptides representing the first repeat (R1) and the first interrepeat (R1-R2 IR) domains. We found that very low molar ratios of tau to tubulin stabilize steady-state dynamics. In addition, both tau peptides stabilize microtubules in a manner similar to that of tau. Tau and the tau peptides reduce the rates and extents of growing and shortening and increase the percentage of time that the microtubules spend in an attenuated state, neither growing nor shortening detectably. The data support a mechanistic model in which binding of tau to tubulin in microtubules stabilizes microtubules in great part by inducing a conformational change in the tubulin that strengthens inter-tubulin bonding.

MATERIALS AND METHODS

Synthesis and Purification of Tau and Tau Peptides. Recombinant full-length adult rat tau protein was synthesized in *Escherichia coli* using the pET vector expression system (Novagen Inc., Madison, WI). Briefly, the coding sequence of the adult rat tau cDNA (Kosik et al., 1989) was subcloned into the *Nde*I site of the pET-3c vector and introduced into BL21 (DE3) cells. Tau protein expression was induced by the addition of 0.4 mM isopropyl β-D-thiogalactopyranoside to cells in log phase growth. Two hours after induction, cells were pelleted and resuspended in 50 mM Pipes (pH 6.8), 1 mM EGTA, and 1 mM $MgCl_2$ (PME buffer) supplemented with 0.1% β-mercaptoethanol and protease inhibitors (PMSF, leupeptin, and pepstatin). Lysozyme was added at 0.1 mg/mL, the cells were incubated at 0 °C for 15 min and sonicated, and the lysates were cleared by centrifugation for 15 min at 4 °C, 18000*g*. Supernatants were boiled

for 5 min and centrifuged as described earlier to clear the cell lysate. Tau was then purified from the supernatant by phosphocellulose column chromatography (Whatman P11). NaCl from the salt wash of the column was removed by exhaustive dialysis against PME buffer supplemented with 0.1% β-mercaptoethanol, and the purified tau protein was concentrated and stored at −70 °C. Tau concentration was determined from the optical density at 278 nm by using an extinction coefficient of 0.29 (Cleveland et al., 1977b).

The octadecapeptide representing R1 (VRSKIGSTENLKHQPGGG), a scrambled form of R1, R1(S) (IHQPGKVTGRSESNGKLG), an octapeptide representing R1-R2 IR (KVQIINKK), and a scrambled and slightly modified form[2] of R1-R2 IR, R1-R2 IR(S) (IKDNVKQILK), were synthesized as described previously on a Millipore 9050-plus peptide synthesizer by DIPCDI/HOBT chemistry (Millipore Corp., Bedford, MA) (Goode & Feinstein, 1994). The peptides were purified to >99% purity by reverse-phase high-pressure liquid chromatography and lyophilized. Peptide sequences were confirmed by mass spectrometry (Goode & Feinstein, 1994).

Purification of Tubulin. Bovine brain microtubule protein was isolated without glycerol by three cycles of polymerization and depolymerization followed by phosphocellulose chromatography as described in Toso et al. (1993). The tubulin solution was quickly frozen as drops in liquid nitrogen and stored at −70 °C until use. Protein concentration was determined by the method of Bradford (1976) using bovine serum albumin as the standard.

Determination of Steady-State Microtubule Polymer Mass in the Presence of Tau, R1, or R1-R2 IR. Tubulin pellets were thawed and centrifuged at 4 °C to remove any aggregated or denatured tubulin. Tubulin (13 μM) was mixed with *Strongylocentrotus purpuratus* flagellar seeds (Toso et al., 1993) in 87 mM Pipes, 36 mM Mes, 1.4 mM $MgCl_2$, and 1 mM EGTA (pH 6.8) (PMME buffer) containing 1 mM GTP and incubated at 37 °C in the absence or presence of different amounts of tau, R1, or R1-R2 IR for 35 min to polymerize the microtubules. The microtubules were pelleted by centrifugation at 150000*g* for 1 h, and the microtubule pellets were solubilized in PMME buffer at 0 °C. The protein concentration was determined (Bradford, 1976), and the soluble tubulin concentration was calculated by subtracting the pellet concentration from the total tubulin concentration.

Video Microscopy. Tubulin was mixed with axoneme seeds and polymerized in PMME buffer containing 1 mM GTP in the presence or absence of tau or tau peptides, as described earlier. The seed concentration was adjusted to achieve 3−6 seeds per microscope field. After assembly to steady state, as determined by light scattering at 350 nm (a maximum of 35 min), 2.5 μL of the microtubule suspension was prepared for video microscopy, and the polymerization dynamics of individual microtubules was recorded at 37 °C as previously described (Panda et al., 1994). Under the conditions used, tubulin does not significantly adhere to the glass surfaces of the coverslips used for microscopy, but MAPs can adhere to glass coverslips (see Pryer et al., 1992), and it is possible that some of the tau or tau peptides may have adhered to the coverslips in the present work. Because tau strongly suppresses dynamics at the low concentrations used in this work, it seems unlikely that a significant quantity of tau adhered to the glass. The tau and tau peptide concentrations reported are the total added concentrations and, thus, represent the maximum quantity of tau available for binding to the microtubule surfaces.

The microtubules, which grew predominantly at the plus ends of the seeds, were observed for a maximum of 45 min after they had reached steady state. We used a computer-based analysis system (a gift from Dr. E. D. Salmon, University of North Carolina, Chapel Hill) to follow microtubule length changes with time. Microtubule length changes were monitored in real time using a mouse-driven cursor, and data points were collected at 3−6 s intervals. Microtubules were measured until they underwent complete depolymerization to the axoneme seed or until the microtubule end became obscured. The length changes undergone by a particular microtubule as a function of time were used to create a life history plot, and the growing and shortening rates were determined by least-squares regression analysis of the data points for each growing or shortening phase. The reported mean growing and shortening rates represent the mean values for all growing and shortening events observed for a particular reaction condition. We considered the microtubule to be in a growing phase if the microtubule increased in length by >0.2 μm at a rate >0.15 μm/min and in a shortening phase if the microtubule decreased in length by >0.2 μm at a rate >0.3 μm/min. Length changes equal to or less than 0.2 μm over the duration of six data points were considered attenuation phases. An average of 25−30 microtubules was measured for each experimental condition.

We calculated the catastrophe frequency (a catastrophe is defined as a transition from the growing or attenuated states to shortening) by dividing the number of catastrophes by the sum of the total time spent in the growing plus attenuation phases for all of the microtubules for a particular condition. The rescue frequency (rescue is the transition from shortening to growing or attenuation, but not new growth from a seed) was calculated by dividing the total number of rescue events by the total time spent in the shortening phase for all microtubules for a particular condition. Due to the stochastic nature of the transitions, the error in the transition frequency was estimated by dividing the frequency by the square root of the number of transitions (Walker et al., 1988).

RESULTS

In this work, we examined the effects on microtubule dynamics at steady state of full-length adult rat tau (containing four tubulin-binding repeats), a peptide corresponding to the first binding repeat (R1, VRSKIGSTENLKHQPGGG), and a peptide corresponding to the interrepeat located between repeats 1 and 2 (R1-R2 IR, KVQIINKK). A schematic representation of full-length tau showing the locations of the R1 and R1-R2 IR domains is shown in Figure 1 (Lee et al., 1988; Goedert et al., 1989 a,b).

[2] Goode and Feinstein (1994) previously demonstrated that the 10-amino acid peptide representing the R1-R2 interrepeat region, KVQIINKKLD, has the ability to promote microtubule polymerization and that a scrambled form of the same peptide, IKDNVKQILK, has no ability to promote microtubule polymerization. Further truncation analysis and mutagenesis showed that the microtubule-binding portion of the peptide resides in the 8-amino acid sequence KVQIINKK. Therefore, in the present work, we used the 8-amino acid peptide KVQIINKK to represent the R1-R2 IR, and we considered the 10-amino acid scrambled peptide IKDNVKQILK as a reasonable negative control. Our observations that the KVQIINKK and KVQIINKKLD peptides both promote tubulin assembly and both suppress microtubule dynamics in our assays (unpublished data) suggest that the two added amino acids, LD, have little or no effect on activity.

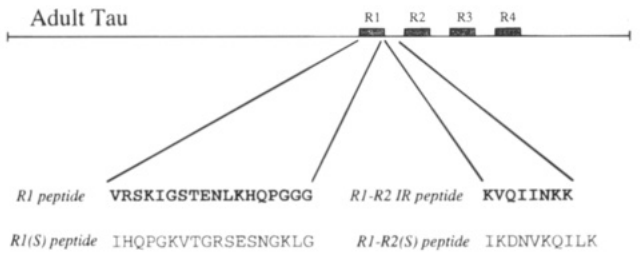

FIGURE 1: Schematic representation of adult (four-repeat) tau. The four tandem repeats, R1, R2, R3, and R4, are marked by bars; the R1-R2 interrepeat is noted by the line between R1 and R2. Amino acid sequences of the peptides used in this study are given; they correspond to specific and scrambled (S) sequences of the repeat 1 domain (R1) and the first interrepeat domain (R1-R2 IR).

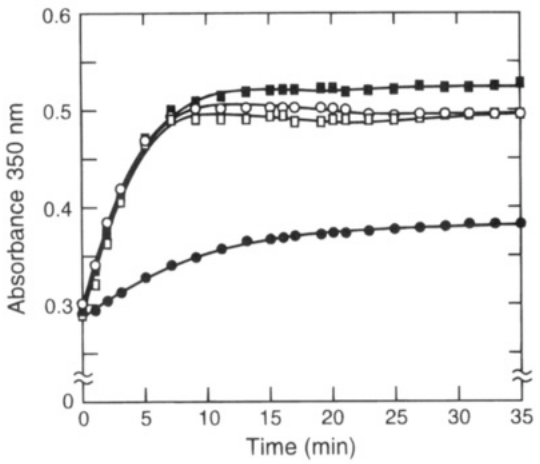

FIGURE 2: Axoneme-seeded microtubule assembly as determined by turbidimetry at 350 nm in the absence or presence of tau, R1, and R1-R2 IR. Purifed bovine brain tubulin (13 μM) was polymerized to steady state at 37 °C in PMME buffer plus 1 mM GTP at the ends of a fixed concentration of axonemal seeds in the absence (●) or presence of 1.2 μM tau (■), 1000 μM R1 (□), or 1000 μM R1-R2 (○) (see Materials and Methods).

Establishment of Steady-State Conditions; Effects of Tau on Steady-State Microtubule Polymer Mass

Tubulin (13 μM) was polymerized to polymer mass steady state in PMME buffer containing 1 mM GTP by incubation with axonemal seeds in the absence or presence of low ratios of tau to tubulin (Materials and Methods). As shown in Figure 2, steady state was attained within 35 min from the time of initiation in either the absence or presence of 1.2 μM tau (ratio of total tau to total tubulin, 1:11), the highest tau to tubulin ratio used in this work. As expected, 1.2 μM tau strongly stimulated the rate and extent of polymerization. In addition, both the rate and extent of polymerization decreased with decreasing tau concentrations (see Table 1), so that at 0.075 μM tau (1:175 tau:tubulin) the extents of polymerization in the presence and absence of tau were indistinguishable. Microtubules attained polymer mass steady state by 35 min of incubation of all tau concentrations used (data not shown).

Suppression of Steady-State Dynamics by Tau

Suppression of Growing and Shortening Rates. Under the conditions used, the microtubules primarily grew at the plus ends of the seeds, as determined by the growth rates, the number of microtubules, and the relative lengths of the microtubules at opposite ends of the seeds (Walker et al., 1988; Pryer et al., 1992; Drechsel et al., 1992; Toso et al., 1993; Panda et al., 1994). Microtubules grew at the minus ends, but under the conditions used, usually no more than one microtubule grew at the minus end of a seed, and clear differences in the growth rates of the microtubules at the two ends were apparent. Control microtubules polymerized to steady state in the absence of tau displayed typical dynamic instability behavior at their plus ends, as shown in the life history traces in Figure 3A. In contrast, the addition of 1.2 μM tau (Figure 3B) strongly suppressed the growing and shortening dynamics.

Table 1: Effects of Tau, R1, and R1−R2 IR on Polymer Mass

A. Tau

concentration (μM)	tau:tubulin molar ratio	tubulin in polymer (μM)	tubulin in solution (μM)
0	0	3.0 ± 0.3	10.0 ± 0.3
0.075	1:175	3.1 ± 0.5	9.9 ± 0.5
0.15	1:85	3.5 ± 0.4	9.5 ± 0.4
0.30	1:45	4.3 ± 0.4	8.7 ± 0.4
0.60	1:22	4.4 ± 0.7	8.6 ± 0.7
1.2	1:11	6.6 ± 0.6	6.4 ± 0.6

B. R1 and R1(S)

concentration (μM)	tubulin in polymer (μM)	tubulin in solution (μM)
0	3.0 ± 0.3	10.0 ± 0.3
250	3.3 ± 0.2	9.7 ± 0.2
500	4.3 ± 0.4	8.7 ± 0.4
1000	5.6 ± 0.3	7.4 ± 0.3
1000 R1(S)	3.2 ± 0.3	9.8 ± 0.3

C. R1−R2 IR and R1−R2(S)

concentration (μM)	tubulin in polymer (μM)	tubulin in solution (μM)
0	3.0 ± 0.3	10.0 ± 0.3
250	3.4 ± 0.7	9.6 ± 0.7
500	4.7 ± 0.5	8.3 ± 0.5
1000	6.2 ± 0.9	6.8 ± 0.9
1000 R1−R2(S)	2.9 ± 0.3	10.1 ± 0.3

The actions of tau at different tau to tubulin ratios (between 1:175 and 1:11) on the individual dynamic instability parameters of steady-state microtubules were determined quantitatively (Table 2A). The mean growing rate for control microtubules in the absence of tau was 1.03 ± 0.41 μm/min. Such large standard deviations in growing (and shortening) rates have been observed previously and may represent intrinsic differences in the polymer structures assembled *in vitro* (Gildersleeve et al., 1992; Drechsel et al., 1992). The addition of tau reduced the growing rate in a concentration-dependent manner. At the lowest ratio of tau to tubulin used (1:175, 0.075 μM tau), the mean growing rate was slightly reduced (10−15%), but the reduction was not statistically significant. However, the mean growing rate was inhibited significantly as the ratio of tau to tubulin was increased. At the highest ratio of tau to tubulin (1:11, 1.2 μM tau), the steady-state mean growing rate was decreased by approximately 40% to 0.58 μm/min (Table 2A). Inhibition of the growing rate by tau correlated well with the ability of tau to reduce the free subunit concentration (Table 1 and Discussion).

Tau also decreased the mean shortening rate (Table 2A). In contrast to the minimal effects that a tau:tubulin ratio of 1:175 (0.075 μM tau) exerted on the growing rate, this ratio of tau to tubulin suppressed the mean shortening rate by approximately 44%, and at the highest tau:tubulin ratio used (1:11, 1.2 μM tau), the shortening rate was reduced by approximately 70%. Histograms of mean shortening rates in the absence or presence of tau are shown in Figure 4.

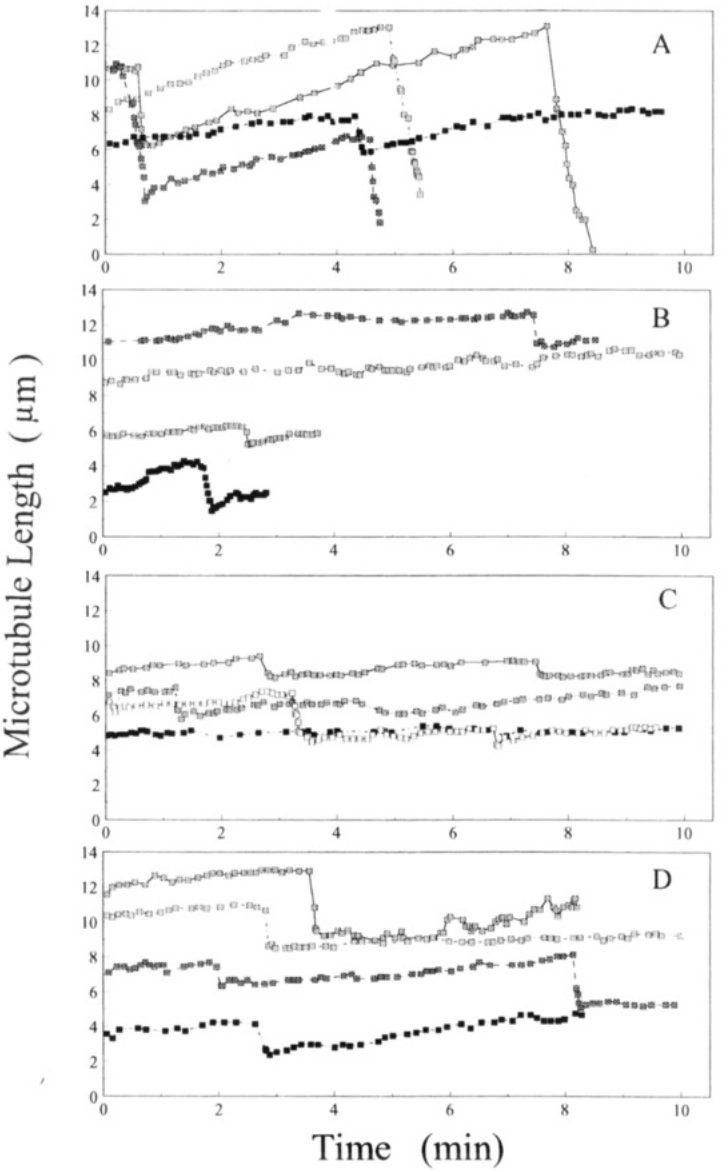

FIGURE 3: Changes in steady-state plus-end microtubule lengths with time in the absence (A) or presence of 1.2 μM tau (B), 1000 μM R1 (C), and 1000 μM R1-R2 IR (D). The life history traces shown are typical examples of individual microtubules growing and shortening.

Tau (1.2 μM) decreased the shortening rates and virtually eliminated the extremely rapid shortening events, thus resulting in substantially narrower shortening rate distributions than in controls (Figure 4B).

We also determined the average length the microtubules shortened per shortening event by dividing the summed shortening lengths for all microtubules for a particular condition by the total number of shortening events for all microtubules measured for that condition. As shown in Figure 5A, tau dramatically reduced the mean shortening length of each shortening event. For example, at a tau to tubulin ratio of 1:175 (0.075 μM tau), the mean shortening length per shortening event decreased by 45% from 6.7 to 3.8 μm. In addition, tau caused a significant reduction in the distribution of shortening lengths per shortening event and a disappearance of the large shortening length excursions (Figure 4E,F). Therefore, the decreases in shortening rate and in the length shortened per shortening event and the tightening of the rate and length distributions by tau indicate that tau increased the structural stability of the microtubules.

Effects of Tau on the Percentage of Time the Microtubules Remain in an Attenuated (Paused) Sta . At or near steady state, microtubules *in vitro* and in cells pend a considerable fraction of the total time in a pause or attenuated phase (Toso et al., 1993; Shelden & Wadsworth, 1993; Panda et al., 1994; Dhamodharan & Wadsworth, 1995). In the attenuated state, subunit addition and loss may be occurring, but the extent of net growth or shortening is too low to be detected by video microscopy. Under the conditions used, the microtubules in the absence of tau spent approximately 5% of the total time in an attenuated state. The percentage of time spent in the attenuated state was significantly increased by tau (Table 2A). For example, at a tau to tubulin ratio of 1:11 (1.2 μM tau), the percentage of time spent in the attenuated state increased from 5% to 33%, a more than 6-fold increase. This increase ccurred in association with a significant decrease in the pe centage of time the microtubules spent shortening and a moderate dec ease in the percentage of time the microtubules spent growing (Table 2A).

Actions of Tau on Transition Frequencies. The catastrophe frequency (frequency of transition to a shortening event) was determin d by dividing the number of catastrophes by the sum of the total time spent growing plus the total time spent in the attenuated phase. The rescue frequency (frequency of transition from shortening to growing or from

Table 2: Effects of Tau, R1, and R1−R2 IR on Steady-State Dynamic Instability Parameters[a]

A. Tau

	concentration (μM)					
	0	0.075	0.15	0.3	0.6	1.2
mean rate (μm/min)						
growing	1.03 ± 0.41	0.85 ± 0.52	0.75 ± 0.61	0.61 ± 0.41	0.62 ± 0.45	0.58 ± 0.45
shortening	16.6 ± 7.6	9.3 ± 7.7	9.3 ± 7.1	6.6 ± 5.8	5.5 ± 5.6	5.2 ± 5.2
total time (%)[b]						
growing	82.9	80.4	78.3	74.1	76.5	61.0
shortening	12.1	11.3	11.3	10.2	5.9	5.8
attenuation	5	8.3	10.4	15.7	17.6	33.2

B. R1 and R1(S)

	concentration (μM)				
	0	250	500	1000	1000 R1(S)
mean rate (μm/min)					
growing	1.03 ± 0.41	0.84 ± 0.53	0.79 ± 0.41	0.56 ± 0.41	0.98 ± 0.74
shortening	16.6 ± 7.6	7.03 ± 6.1	6.21 ± 6.6	5.1 ± 5.8	17.5 ± 5.6
total time (%)[b]					
growing	82.9	70.3	73.8	75.0	84.4
shortening	12.1	11.1	9.2	6.9	11.2
attenuation	5.0	18.6	17.0	18.1	4.4

C. R1−R2 IR and R1−R2(S)

	concentration (μM)				
	0	250	500	1000	1000 R1−R2(S)
mean rate (μm/min)					
growing	1.03 ± 0.41	0.89 ± 0.56	0.73 ± 0.42	0.66 ± 0.38	0.95 ± 0.60
shortening	16.6 ± 7.6	11.1 ± 8.7	10.5 ± 10.1	8.45 ± 6.6	14.4 ± 8.7
total time (%)[b]					
growing	82.9	77.2	77.0	74.5	75.7
shortening	12.1	11.9	9.1	8.8	13.8
attenuation	5	10.9	13.9	16.7	10.5

[a] Values are mean ± the standard deviation. [b] If one determines the changes in microtubule length of MAP-free microtubules on the basis of the dynamics data obtained in this study, it would appear that the microtubules were undergoing net depolymerization rather than being at steady state. However, this is due to the method of analysis, which slightly underestimates the percentage of total time that the microtubules grow and overestimates the percentage of time the microtubules spend shortening. In fact, in most studies *in vivo* (e.g., Dhamodhran & Wadsworth, 1995) and *in vitro* (e.g., Walker et al., 1988; Pryer et al., 1992; Trinzeck et al., 1993; Itoh & Hotani, 1994), the method used results in the calculated net shortening of plus ends. The reason is that one must begin measurement with a microtubule that has already attained a certain length. The rescue frequency is low in the absence of MAPs, and therefore microtubules will often undergo complete depolymerization after a catastrophe. Thus, the observer measures more microtubule length lost than gained. When MAPs are present and the microtubules do not depolymerize significantly due to increased rescue frequency, shortening and growing are balanced.

shortening to the attenuated state) was calculated by dividing the number of rescue events by the total time spent in the shortening phase. As shown in Table 3A, 1.2 μM tau decreased the catastrophe frequency by ~35%, whereas the increase in rescue frequency was dramatic (~350%).

The ability of tau to increase the rescue frequency could be due to the reduction in the shortening rate rather than to a direct effect on cap stabilization. In support of this possibility, we found that the rescue frequency increased linearly with the inverse of the shortening rate (data not shown). We also calculated the rescue frequency in the manner described by Kowalski and Williams (1993) by dividing the total number of rescues by the total length shortened during a shortening event. The rescue frequency per micrometer of shortening is shown as a function of tau concentration in Figure 6A; tau strongly increased the frequency of rescue per micrometer of shortening. For example, a tau to tubulin ratio of 1:11 (1.2 μM tau) increased the rescue frequency by approximately 9.5-fold (Figure 6A). Together with the results indicating that tau does not strongly affect the catastrophe frequency, the data indicate that tau does not directly stabilize the cap, but rather it increases the rescue frequency by slowing the shortening rate and decreasing the extent of each shortening excursion.

Stabilization of Steady-State Microtubule Dynamics by the Microtubule-Binding Domains of Tau

To dissect the molecular mechanisms by which intact tau affects microtubule dynamics, we examined the actions on the dynamics of peptides corresponding to two different tubulin-binding domains in tau. Consistent with previous studies (Ennulat et at., 1989; Maccioni et al., 1989; Goode & Feinstein, 1994), high concentrations of the R1 and R1-R2 IR peptides were required to stimulate tubulin polymerization (Figure 2 and Table 1), which likely reflects the weaker binding affinity of these peptides for tubulin than for tau. As with full-length adult tau, the steady state was attained by 35 min of incubation (Figure 2). Interestingly, R1 and R1-R2 IR both suppressed steady-state microtubule dynamics in a manner that was qualitatively indistinguishable from intact tau (Figure 3C,D).

Suppression of Growing and Shortening Rates by R1 and R1-R2 IR. R1 and R1-R2 IR reduced both the mean growing and shortening rates at steady state in a concentration-dependent manner. As with full-length tau, the effects of the peptides on the mean shortening rate were much stronger than the effects on the growing rate (Table 2B,C). For example, 250 μM R1 reduced the mean shortening rate by 58% from 16.6 to 5.2 μm/min, while the mean growing rate

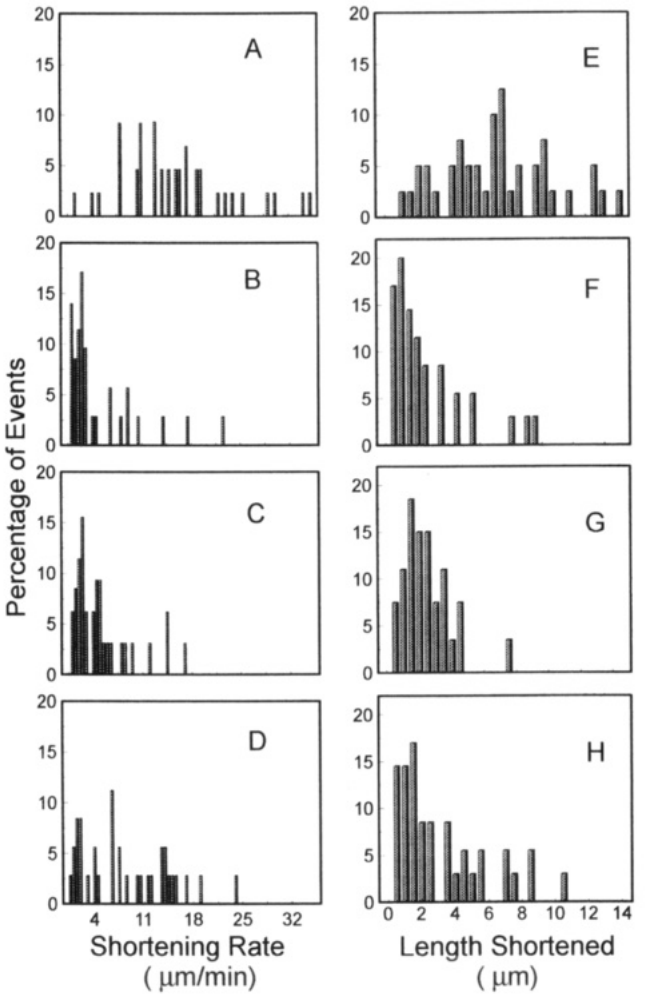

FIGURE 4: Frequency histograms of microtubule shortening rates and the length shortened per shortening event at steady state in the absence or presence of 1.2 μM tau, 1000 μM R1, and 1000 μM R1-R2 IR. Shortening rates and lengths were determined as described in Materials and Methods. Shown here are shortening rate distribution histograms for control microtubules (A), tau (B), R1 (C), and R1-R2 (D) and shortening length distribution histograms for control microtubules (E), tau (F), R1 (G), and R1-R2 IR (H).

was reduced by only 15%. The effects of R1-R2 IR on the rates of growing and shortening were qualitatively similar to those of R1, but R1-R2 IR was somewhat less potent than R1. For example, 1000 μM R1 inhibited the shortening rate by 69%, whereas 1000 μM R1-R2 IR inhibited the shortening rate by 49% (Table 2B,C). Similar to the effects of tau, R1 (1000 μM) and R1-R2 IR (1000 μM) eliminated the extremely rapid shortening events, which resulted in substantially narrower shortening rate distributions (Figure 4C,D). R1 and R1-R2 IR also decreased the length of microtubule lost per shortening event, as shown in Figure 5B. For example, at 1000 μM R1 or R1-R2 IR, the mean shortening length decreased by 3.2- or 2.2-fold, respectively. Also, R1 and R1-R2 IR significantly reduced the distribution of shortening lengths per shortening event (Figure 4G,H).

Effects of R1 and R1-R2 IR on the Percentage of Time Spent in the Attenuated State and on Transition Frequencies. Like full-length tau, the R1 and R1-R2 IR peptides also reduced the percentage of time that the microtubules spent growing and shortening and increased the percentage of time that the microtubules spent in an attenuated state (Table 2B,C). For example, 1000 μM R1 increased the percentage of time spent in the attenuated state by approximately 3-fold

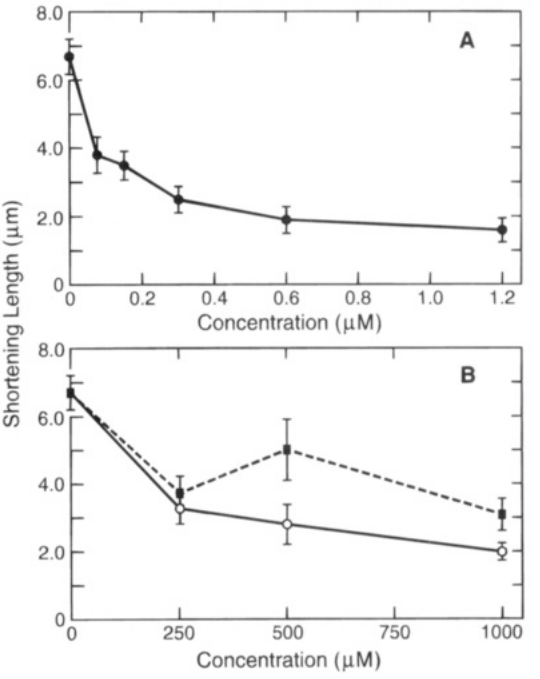

FIGURE 5: Suppression of the shortening length per shortening event at plus ends of steady-state microtubules by tau, R1, and R1-R2 IR. The length shortened per shortening event was calculated by dividing the total shortening length by the total number of shortening events for all microtubules measured: (A) tau (B) R1 (○) and R1-R2 IR (■). Error bars represent the standard error of the mean.

Table 3: Effects of Tau, R1, and R1−R2 IR on Transition Frequencies[a]

A. Tau

concentration (μM)	tau:tubulin ratio	catastrophes/min	rescues/min
0	0	0.32 ± 0.05	0.92 ± 0.22
0.075	1:175	0.32 ± 0.05	1.85 ± 0.38
0.15	1:85	0.31 ± 0.05	1.85 ± 0.32
0.30	1:45	0.26 ± 0.04	2.00 ± 0.32
0.60	1:22	0.19 ± 0.03	2.70 ± 0.45
1.20	1:11	0.21 ± 0.04	3.15 ± 0.57

B. R1 and R1(S)

concentration (μM)	catastrophes/min	rescues/min
0	0.32 ± 0.05	0.92 ± 0.22
250	0.25 ± 0.04	1.90 ± 0.30
500	0.22 ± 0.04	1.95 ± 0.32
1000	0.17 ± 0.03	2.17 ± 0.42
1000 R1(S)	0.34 ± 0.05	1.07 ± 0.25

C. R1−R2 IR and R1−R2(S)

concentration (μM)	catastrophes/min	rescues/min
0	0.32 ± 0.05	0.92 ± 0.22
250	0.36 ± 0.06	1.70 ± 0.36
500	0.22 ± 0.04	1.60 ± 0.33
1000	0.25 ± 0.04	2.08 ± 0.38
1000 R1−R2 IR(S)	0.39 ± 0.07	1.04 ± 0.20

[a] Values are mean ± standard error (Walker et al., 1988); mean of approximately 35 events per condition.

from 5% to 18.1%. The potency of R1 was only minimally greater than that of R1-R2 IR. Similar to the action of full-length tau, 1000 μM R1 and R1-R2 IR moderately reduced the catastrophe frequency and strongly increased the rescue frequency (Table 3B,D and Figure 6B).

Specificity of R1 and R1-R2 IR. To determine whether the ability of R1 or R1-R2 IR to stabilize microtubule dynamics was sequence specific, we synthesized a scrambled form of R1, called R1(S) (IHQPGKVTGRSESNGKLG), and

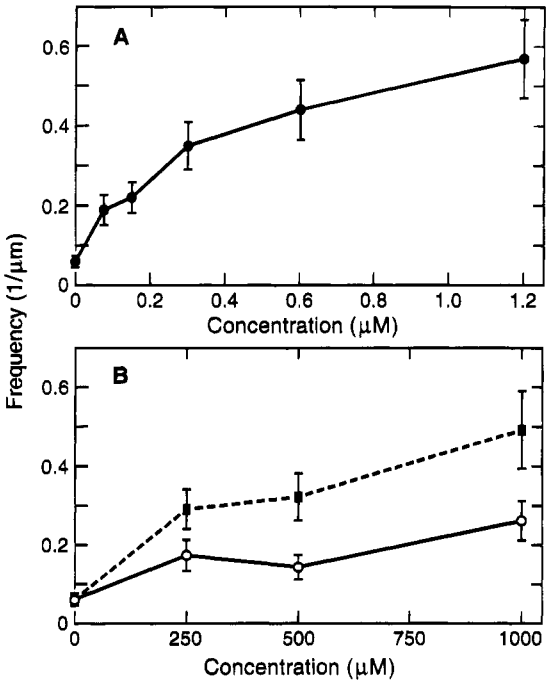

FIGURE 6: Increase in rescue frequency per micrometer of length shortened with increasing concentrations of tau (A), R1 (B, ■), and R1-R2 IR (B, O). The rescue frequencies were calculated by dividing the total number of rescues by the total shortening lengths for all microtubules. Error bars represent standard deviation.

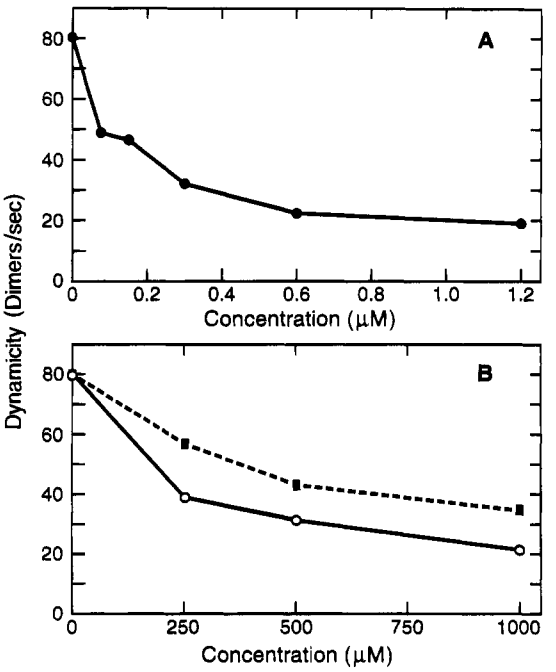

FIGURE 7: Suppression of steady-state microtubule dynamicity by tau (A), R1 (B, O), and R1-R2 IR (B, ■). Dynamicity (Materials and Methods) is the overall tubulin dimer exchange per second.

used a scrambled form of R1-R2 IR, called R1-R2 IR(S) (IKDNVKQILK) (Goode and Feinstein, 1994), in which the amino acid sequences of the two peptides were randomly altered. At concentrations of 1000 μM, both R1(S) and R1-R2 IR(S) had little or no effect on microtubule dynamics. The actions of the scrambled peptides on the growing or shortening rates or on the percentage of time the microtubules spent growing, shortening, or in the attenuated state (Table 2B,C) were all within 10% of control values.

Effects of Tau, R1, and R1-R2 IR on Overall Dynamicity at Steady State. Dynamicity, which is calculated from all detectable growth and shortening events, including the time spent in the attenuated state, provides a measure of overall dimer exchange at steady state (Toso et al., 1993; Panda et al., 1994). Decreased dynamicity indicates increased stability. As shown in Figure 7, tau, R1, and R1-R2 IR strongly reduced dynamicity. At the highest concentrations examined, tau, R1, and R1-R2 IR inhibited dynamicity by 75%, 75%, and 56%, respectively.

DISCUSSION

The present work on the action of tau and tau peptides on microtubule dynamic instability was carried out at polymer mass steady state, which may reflect the conditions in mature axons. We found that low ratios of tau to tubulin, between 1:175 and 1:11, which spanned those found in undifferentiated and differentiated PC-12 cells (Drubin et al., 1985), reduced the rate and extent of shortening. In contrast to the action of tau under conditions of net polymer gain (Pryer et al., 1992; Drechsel et al., 1992), these low ratios of tau to tubulin also decreased the rate and extent of growth. Tau also strongly increased the percentage of time microtubules spent in an attenuated state, neither growing nor shortening detectably, and increased the rescue frequency. At the lowest ratios of tau to tubulin used, suppression of dynamics occurred with minimal increases in polymer mass, and at the highest ratio of tau to tubulin used (1:11, 1.2 μM tau), the critical subunit concentration was decreased by only 40%. Thus, under steady-state conditions, relatively low molar ratios of tau to tubulin kinetically stabilize microtubule dynamics in the absence of strong increases in polymer mass. In addition, R1 and R1-R2 IR qualitatively mimicked the action of full-length tau, although the potency of the peptides was approximately 1000-fold lower on a molar basis than that of full-length tau.

Substoichiometric Molar Ratios of Tau to Tubulin Kinetically Stabilize Microtubule Growing and Shortening Dynamics

Suppression of Steady-State Shortening by Tau. Low molar ratios of tau to tubulin did not strongly inhibit the catastrophe frequency; thus, it was possible to examine the actions of tau on microtubule shortening. We found that low ratios of tau to tubulin strongly reduced both the steady-state shortening rate and length shortened during a shortening event (Table 2 and Figure 5). This appears to be the primary mechanism responsible for microtubule stabilization by tau. These results are in accord with previous studies carried out *in vitro* on the effects of unfractionated brain MAPs or MAP2 on the dynamics of individual microtubules, which have shown that the MAPs strongly reduce both the rate and extent of shortening (Horio & Hotani, 1986; Pryer et al., 1992; Toso et al., 1993; Kowalski & Williams, 1993). Drechsel et al. (1992), using dark-field microscopy, were unable to measure shortening events under conditions of microtubule elongation in the presence of tau, because at the conditions used the catastrophe frequency was too low. However, they could show that tau reduced the shortening rate of individual microtubules under conditions in which the tubulin concentration was lowered by perfusion with tubulin-free buffer.

Tau Increases the Percentage of Time Microtubules Spend in the Attenuated State. Microtubules *in vivo* spend a significant fraction of their total time in an attenuated or

pause state, when neither growth nor shortening can be detected by video microscopy (Sammak & Borisy, 1988; Shelden & Wadsworth, 1993; Dhamodharan & Wadsworth, 1995). Similarly, microtubules also spend considerable time in an attenuated state *in vitro* at steady state (Toso et al., 1993; Panda et al., 1994; Derry et al., 1995) whereas under non-steady-state conditions, microtubules spend very little time in the pause or attenuated state (Walker et al., 1988). In the present work, we found that tau significantly increased the percentage of time that the microtubules spent in the attenuated state (Table 2A), thus further indicating that tau kinetically stabilizes microtubule dynamics.

Suppression of Steady-State Growing Rates; Correlation with the Reduction in the Tubulin Concentration. At polymer mass steady state, tau decreased plus-end growing rates (Table 2A). Such data might appear to be incompatible with the results of previous studies in which tau increased growing rates (Pryer et al., 1992; Drechsel et al., 1992). However, the present studies were carried out at steady state, and the results of Pryer et al. (1992) and Drechsel et al. (1992) were carried out under conditions of net polymer gain.

The growing rate at a microtubule end depends on the association rate constant, the concentration of free tubulin, and the dissociation rate constant, according to the following relationship:

$$r_g = k_+C - k_- \quad (1)$$

where r_g is the growing rate, k_+ is the association rate constant, k_- is the dissociation rate constant, and C is the soluble tubulin concentration. Under the reaction conditions used in the present study, tau did not appreciably reduce the growing rate at the lowest concentration used and did not appreciably reduce the critical concentration at this tau concentration. As the tau concentration was increased, the soluble tubulin level decreased concomitant with the decrease in growing rate. At the highest tau concentration used (1.2 μM), the soluble tubulin concentration was reduced by approximately 40% from 10 to 6.4 μM concomitant with a 40% reduction in the growing rate (Tables 1 and 2). Thus, the reduction in the mean growing rate at steady state by tau can be accounted for by the reduction in the soluble tubulin concentration. A similar reduction in the growing rate was obtained when the growing rates of individual MAP-rich microtubules were compared with those of MAP-free microtubules at steady state *in vitro* (Toso et al., 1993) and when heat-stable MAPs and MAP2 were microinjected into living cultured BSC-1 cells, which also, presumably, were at or close to steady state (Dhamodhoran & Wadsworth, 1995). Under conditions of rapid elongation, Drechsel et al. (1992) obtained evidence indicating that tau may actually increase the association rate constant for tubulin addition at microtubule plus ends. However, several investigators (Bré & Karsenti, 1990; Pryer et al., 1992) concluded that the ability of tau to increase the apparent growing rates was due to a decrease in the dissociation rate constant rather than to an increase in the association rate constant. In the present work, at low ratios of tau to tubulin at steady state, no increase in the association rate constant was detectable.

Effects of Tau on the Transition Frequencies. The effects of tau on the steady-state catastrophe frequency were negligible at low molar ratios of tau to tubulin (at or below 0.15 μM, Table 3A) and were relatively modest even at high ratios of tau to tubulin. For example, only a 35% decrease in the catastrophe frequency occurred at a molar ratio of tau to tubulin of 1:11 (1.2 μM tau), which was the highest ratio examined. Similar results were obtained by Dhamordharan and Wadsworth (1995) when heat-stable MAPs were injected into cultured BSC-1 cells. However, Drechsel et al. (1992) observed a large decrease in the catastrophe frequency at high ratios of tau to tubulin under conditions of rapid polymer gain. Such data might be taken to indicate that tau acts directly on the stabilizing cap, increasing its retention. However, as previously suggested by Drechsel et al. (1992), a decrease in the catastrophe frequency by tau may not be due to a direct action of tau on the stabilizing cap. One possibility is that the binding of large numbers of tau molecules along the microtubule lattice decreases the rate and extent of shortening to such an extent that catastrophes are too small to be detected by video microscopy. Both Walker et al. (1988) and Drechsel et al. (1992) observed that the catastrophe frequency decreased with increased growing rate and increased soluble tubulin concentration. Thus, one reason why tau may not have strongly suppressed the catastrophe frequency in the present work may be that the suppression was masked by the decreased growing rate and decreased soluble tubulin concentration.

Microtubules that assembled to polymer mass steady state in the presence of tau persisted substantially longer than microtubules assembled with purified tubulin, in large part because tau strongly increased the rescue frequency (Table 3). Similar results have been reported by Pryer et al. (1992) and Drechsel et al. (1992) under conditions of net polymer gain. However, similar to the effects of tau that have been observed on the catastrophe frequency, the ability of tau to increase the rescue frequency does not necessarily indicate that tau is directly increasing the frequency of cap regain. It seems more likely that because tubulin dissociation during shortening was strongly slowed by tau, there was a greatly increased opportunity for regain of the stabilizing cap. This idea is supported by the data indicating that the dependence of the rescue frequency was linearly proportional to the inverse of the shortening rate and also that increasing concentrations of tau significantly increased the rescue frequency per unit length shortened (Table 2 and Figure 6). Thus, it is expected that high ratios of tau to tubulin would increase the rescue frequency per unit length shortened to such an extent that catastrophe would be undetectable by video microscopy.

Both the R1 and R1-R2 IR Microtubule-Binding Domains Mimic the Action of Intact Tau on Microtubule Polymerization and Steady-State Dynamics

We found that the R1 and R1-R2 IR peptides stimulated microtubule assembly (Figure 2) and kinetically stabilized microtubule dynamics in a manner that was qualitatively very similar to the action of full-length adult tau. The present results support the conclusions of Goode and Feinstein (1994) that the R1-R2 interrepeat sequence does indeed bind microtubules and stimulates microtubule polymerization. Specifically, both the R1 and R1-R2 IR peptides decreased the growing and shortening rates, reduced the length shortened during a shortening phase, and increased the rescue frequency. Both peptides markedly increased the percentage of time that the microtubules spent in the attenuated state, and like full-length tau, they decreased the overall dynamicity of the microtubules. In addition, R1 was generally more effective than R1-R2 IR (Tables 1B,C and 2B,C).

These results are consistent with earlier reports indicating that small single-peptide sequences representing tubulin-binding domains of tau or MAP2 require at least 2 orders of magnitude higher concentration than full-length tau to promote bulk phase microtubule assembly (Aizawa et al., 1989; Ennulat et al., 1989; Maccioni et al., 1989; Butner & Kirschner, 1991; Goode & Feinstein, 1994). Full-length tau has multiple tubulin-binding sites, and cooperation between these sites may provide intact tau with a more favorable microtubule binding conformation than the synthetic peptides can achieve by themselves. Consistent with previous reports (Maccioni et al., 1989; Ennulat et al., 1989; Goode & Feinstein, 1994), the results indicate that the interaction between the peptides and the tubulin involves not only electrostatic charge neutralization but also a sequence-specific interaction.

A Model for Kinetic Stabilization of Microtubules by Tau

Tau shares homology in its microtubule-binding regions with at least two other MAPs, MAP2 and MAP4. Each is capable of interacting with tubulin through its proline-rich middle region and its carboxyl terminus containing multiple copies of the 18-amino acid repeat (Aizawa et al., 1991; Lewis et al., 1988, 1989; Butner & Kirschner, 1991; Chapin & Bulinski, 1992; Yamauchi et al., 1993; Goode & Feinstein, 1994; Gustke et al., 1994). In addition to the homology among repeats, the R1-R2 IR domain is highly conserved among these MAPs (Goedert et al., 1989a,b; Lewis et al., 1988; Lee et al., 1988), raising the possibility that it performs a similar microtubule-binding function in MAP2 and MAP4 (specifically, in isoforms containing >3 repeats).

A major cognate binding site for these MAPs appears to be in the C-terminus of tubulin, because removal of the C-terminus by digestion with subtilisin results in the loss of MAP binding activity and an inability of the MAPs to stimulate polymerization (Serrano et al., 1984; Littauer et al., 1986). Data indicating that the maximal stoichiometry of tau binding to tubulin is approximately 1:5, together with the theoretical possibility that the interrepeat segments can span the distance between subunits, have given rise to the idea that each tau repeat might bind to a different turbulin monomer (Hirokawa et al., 1988; Butner & Kirschner, 1991). This model helps to explain the ability of full-length tau to stabilize microtubules: it suggests that lateral interprotofilament associations and/or longitudinal dimer associations are stabilized by tau binding to multiple tubulin subunits in the lattice.

However, our results suggest that tau may stabilize microtubules by a different primary mechanism. The R1 and R1-R2 IR peptides, which represent single microtubule-binding domains as short as 8 amino acids in length, kinetically stabilized steady-state microtubule dynamics in a manner that was qualitatively similar to full-length tau. By assuming that these short peptides are not capable of spanning multiple tubulin subunits in the lattice, it seems like that the stabilizing activity of tau is due in large part to an ability to strengthen inter-tubulin bonding by inducing a conformational change in the tubulin. While the multiple repeats of tau may still be involved in microtubule stabilization, it follows that the main purpose of the multiple binding repeats may be to increase the affinity of tau (or other MAPs with similar multiple binding repeats) for the microtubule surface.

That the R1 and R1-R2 IR peptides influence microtubule dynamics similarly to one another is surprising. Results of binding competition assays have indicated that the R1 and R1-R2 IR domains in tau may bind to distinct sites in tubulin (Goode & Feinstein, 1994). In addition, the peptides appear to interact with tubulin via different molecular mechanisms. Whereas the repeats derive their binding energies from a distributed array of weak sites involving van der Waals and/or highly shielded ionic forces (Butner & Kirschner, 1991), R1-R2 IR appears to derive its binding energy from two well-defined lysine residues, implicating strong ionic interactions with tubulin (Goode & Feinstein, 1994). Binding of R1 and R1-R2 IR to different tubulin-binding sites might be expected to give rise to different effects on microtubule dynamic parameters. Yet, in this study, the actions of the two peptides on dynamics were qualitatively similar (and similar to that of full-length tau).

It is also intriguing that the drug taxol exerts actions on bulk microtubule polymerization and on the growing and shortening dynamics of individual microtubules at steady state that are remarkably similar to the actions of tau and two different tau peptide domains. In bulk solution, taxol stimulates microtubule nucleation, promotes microtubule elongation, and strongly stabilizes microtubules (Schiff et al., 1979; Caplow & Zeeberg, 1982; Wilson et al., 1985; Derry et al., 1995). In addition, analysis of the effects of taxol on the growing and shortening dynamics of MAP-depleted microtubules at steady state *in vitro* by video microscopy indicates that, at the lowest effective drug concentrations, taxol suppressed the rate and extent of microtubule shortening concomitant with a moderate reduction in the critical concentration. Like the action of tau, taxol also strongly increased the percentage of time that microtubules spend in an attenuated state, neither growing nor shortening detectably (Derry et al., 1995). Interestingly, the binding sites for taxol and tau appear to be distinct, on the basis of chemical cross-linking studies with photoaffinity taxol derivatives (Rao et al., 1994) and evidence indicating that tau can bind to its tubulin-binding sites on taxol-stabilized microtubules (Butner & Kirschner, 1991). Chemical cross-linking studies have indicated that the taxol-binding site is at the N-terminus of β-tubulin (Rao et al., 1994). Thus, a qualitatively similar kinetic stabilization of microtubule dynamics can occur by the interaction of molecules with several different regions of tubulin exposed at the microtubule surface.

Finally, the finding that the R1 and R1-R2 IR peptides modulate microtubule dynamics in a manner qualitatively similar to the action of full-length adult tau suggests a possible route for preparing low molecular mass stabilizers of microtubule dynamics. It may eventually be possible to generate small peptides having high microtubule binding affinity that have much smaller (taxol-like) microtubule-stabilizing activity than R1 or R1-R2 IR.

ACKNOWLEDGMENT

We thank Mr. Herb Miller for preparing the bovine brain tubulin used in this work and Joe McCarty for providing recombinant full-length tau. We thank Mr. Brent Derry, Ms. Cindy Dougherty, and Dr. Douglas Thrower for critically reading the manuscript and Ms. Janet Daijo for technical help. We are also grateful to Dr. Monte Radeke and the UCSB Advanced Instrumentation Center for synthesizing the peptides. The UCSB Advanced Instrumentation Center is part of the MRL Central Facilities, supported by the National Science Foundation under Award No. DMR-9123048.

REFERENCES

Aizawa, H., Kawasaki, H., Murofushi, H., Kotani, S., Suzuki, K., & Sakai, H. (1989) *J. Biol. Chem. 264*, 5885−5890.

Aizawa, H., Emori, Y., Mori, A., Murofushi, H., Sakai, H., & Suzuki, K. (1991) *J. Biol. Chem. 266*, 9841−9846.

Bamburg, J. R., Bray, D., & Chapman, K. (1986) *Nature (London) 321*, 788−790.

Bass, P. W., & Black, M. M. (1990) *J. Cell Biol. 111*, 495−509.

Bass, P. W., Pienkowski, T. P., Cimbalnik, K. A., Toyama, K., Bakalis, S., Ahmad, F. J., & Kosik, K. S. (1994) *J. Cell Sci. 107*, 135−143.

Binder, L. I., Frankfurther, A., & Rebhun, L. I. (1985) *J. Cell Biol. 101*, 1371−1378.

Bradford, M. M. (1976) *Anal. Biochem. 72*, 248−254.

Brandt, L., & Lee, G. (1993) *J. Biol. Chem. 268*, 3414−3419.

Bré, M. H., & Karsenti, E. (1990) *Cell Motil. Cytoskel. 15*, 88−98.

Butler, M., & Shelanski, M. L. (1986) *J. Neurochem. 47*, 1517−1522.

Butner, K. A., & Kirschner, M. W. (1991) *J. Cell Biol. 115*, 717−730.

Caceres, A., & Kosik, K. S. (1990) *Nature (London) 343*, 461−463.

Caplow, M., & Zeeberg, B. (1982) *Eur. J. Biochem. 127*, 319−324.

Carlier, M.-F. (1989) *Int. Rev. Cytol. 115*, 139−170.

Chapin, S. J., & Bulinski, J. C. (1992) *Cell Motil. Cytoskel. 23*, 236−243.

Cleveland, D. W., Hwo, S. Y., & Kirschner, M. W. (1977a) *J. Mol. Biol. 116*, 207−225.

Cleveland, D. W., Hwo, S. Y., & Kirschner, M. W. (1977b) *J. Mol. Biol. 116*, 227−247.

Desai, A., & Mitchison, T. J. (1995) *J. Cell Biol. 128*, 1−4.

Derry, W. B., Wilson, L., & Jordan, M. A. (1995) *Biochemistry 34*, 2203−2211.

Dhamodharan, R., & Wadsworth, P. (1995) *J. Cell Sci. 108*, 1679−1689.

Diaz-Nido, J., Hernandez, M. A., & Avila, J. (1990) *Microtubule Proteins* (Avila, J., Ed.) pp 193−257, CRC Press, Inc., Boca Raton, FL.

Donoso, J. A. (1986) *J. Neurobiol. 17*, 383−403.

Drechsel, D. N., Hyman, A. A., Cobb, M. H., & Kirschner, M. W. (1992) *Mol. Biol. Cell 3*, 1141−1154.

Drubin, D., & Kirschner, M. W. (1986) *J. Cell Biol. 103*, 2739−2746.

Drubin, D. G., Feinstein, S. C., Shooter, E. M., & Kirschner, M. W. (1985) *J. Cell Biol. 101*, 1799−1807.

Drubin, D., Kobayashi, S., & Kirschner, M. W. (1986) *Ann. N.Y. Acad. Sci. 466*, 257−268.

Dustin, P. (1984) *Microtubules*, 2nd ed., Springer, Berlin.

Ennulat, D. J., Liem, R. K. H., Hashim, G. A., & Shelanski, M. L. (1989) *J. Biol. Chem. 264*, 5327−5330.

Erickson, H. P., & O'Brien, E. T. (1992) *Annu. Rev. Biophys. Biomol. Struct. 21*, 145−166.

Esmaeli-Azad, B., McCarty, J. H., & Feinstein, S. C. (1994) *J. Cell Sci. 107*, 869−879.

Farrell, K. W., Jordan, M. A., Miller, H. P., & Wilson L. (1987) *J. Cell Biol. 184*, 1035−1046.

Gildersleeve, R. F., Cross, A. L., Cullen, K. E., Fagen, A. P., & Williams, R. C. (1992) *J. Biol. Chem. 267*, 7995−8006.

Goedert, M., Spillantini, M. G., Jakes, R., Rutherford, D., & Crowther, R. A. (1989a) *Neuron 3*, 519−526.

Goedert, M., Spillantini, M. G., Potier, M. C., Ulrich, J., & Crowther, R. A. (1989b) *EMBO J. 8*, 393−399.

Goedert, M., Jakes, R., Spillantini, M. G., & Crowther, R. A. (1994) in *Microtubules* (Hyams, J., & Lloyd, C., Eds.) pp 183−200, Wiley-Liss, New York.

Goode, B. L., & Feinstein, S. C. (1994) *J. Cell Biol. 124*, 769−782.

Grundke-Ikbal, I., Iqbal, K., Tung, Y. M., Quinlan, M., Wisniewski, H. M., & Binder, L. I. (1986) *Proc. Natl. Acad. Sci. U.S.A. 83*, 4913−4917.

Gustke, N., Trinczek, B., Biernat, J., Mandelkow, E.-M., & Mandelkow, E. (1994) *Biochemistry 33*, 9511−9522.

Himmler, A. (1989) *Mol. Cell. Biol. 9*, 1389−1396.

Himmler, A., Drechsel, D., Kirschner, M. W., & Martin, D. W., Jr. (1989) *Mol. Cell. Biol. 9*, 1381−1388.

Hirokawa, N., Shiomura, Y., & Okabe, S. (1988) *J. Cell Biol. 107*, 1449−1459.

Horio, T., & Hotani, H. (1986) *Nature 321*, 605−607.

Hotani, H., & Horio, T. (1988) *Cell. Motil. Cytoskel. 10*, 229−236.

Itoh, T. J., & Hotani, H. (1994) *Cell Struct. Funct. 19*, 279−290.

Kosik, K. S., & Finch, E. A. (1987) *J. Neurosci. 7*, 3142−3153.

Kosik, K. S., & Caceres, A. (1991) *J. Cell Sci. (Suppl.) 15*, 69−74.

Kosik, K. S., Orecchio, L. D., Bakalis, S., & Neve, R. L. (1989) *Neuron 2*, 1389−1397.

Kowalski, R. J., & Williams, R. C. (1993) *J. Biol. Chem. 268*, 9847−9855.

Lee, G., Cowan, N., & Kirschner, M. W. (1988) *Science 239*, 285−288.

Lee, G., Neve, R. L., & Kosik, K. S. (1989) *Neuron 2*, 1615−1624.

Lewis, S. A., Wang, D., & Cowan, N. J. (1988) *Science 242*, 936−939.

Lewis, S. A., Ivanov, I. E., Lee, G. H., & Cowan, N. J. (1989) *Nature (London) 342*, 498−505.

Littauer, U. Z., Giveon, D., Thierauf, M., Ginzburg, I., & Ponstingl, H. (1986) *Proc. Natl. Acad. Sci. U.S.A. 83*, 7162−7166.

Maccioni, R. B., Vera, J. C., Dominguez, J., & Avila, J. (1989) *Arch. Biochem. Biophys. 190*, 809−819.

Margolis, R. L., & Wilson, L. (1978) *Cell 13*, 1−8.

McIntosh, J. R. (1994) *Microtubules* (Hyams, J., & Lloyd, C., Eds.) pp 413−434, Wiley-Liss, New York.

Mitchison, T. J. (1989) *J. Cell Biol. 114*, 637−652.

Mitchison, T., & Kirschner, M. W. (1984) *Nature (London) 312*, 237−242.

Okabe, S., & Hirokawa, N. (1988) *J. Cell Biol. 107*, 651−664.

Okabe, S., & Hirokawa, N. (1990) *Nature (London) 343*, 479−482.

Panda, D., Miller, H. P., Banerjee, A., Luduena, R. F., & Wilson, L. (1994) *Proc. Natl. Acad. Sci. U.S.A. 91*, 11358−11362.

Pryer, N. K., Walker, R. A., Bourns, B. D., Soboeiro, M. F., & Salmon, E. D. (1992) *J. Cell Sci. 103*, 965−976.

Rao, S., Krauss, N. E., Heerding, J. M., Swindell, C. S., Ringel, I., Orr, G. A., & Horwitz, S. B. (1994) *J. Biol. Chem. 269*, 3132−3134.

Sammak, P. J., & Borisy, G. G. (1988) *Nature (London) 332*, 724−726.

Sawin, K. E., & Mitchison, T. J. (1991) *J. Cell Biol. 112*, 941−954.

Schiff, P. B., Fant, J., & Horwitz, S. B. (1979) *Nature (London) 277*, 665−667.

Serrano, L., de la Torre, J., Maccioni, R. B., & Avila, J. (1984) *Proc. Natl. Acad. Sci. U.S.A. 81*, 5989−5993.

Shelden, E., & Wadsworth, P. (1993) *J. Cell Biol. 120*, 935−945.

Tanaka, E., & Kirschner, M. W. (1991) *J. Cell Biol. 115*, 345−363.

Tanaka, E., Ho, T., & Kirschner, M. W. (1995) *J. Cell Biol. 128*, 139−155.

Toso, R. J., Jordan, M. A., Farrell, K. W., Matsumoto, B., & Wilson, L. (1993) *Biochemistry 32*, 1285−1293.

Trinczeck, B., Marx, A., Mandelkow, E.-M., Murphy, D. B., & Mandelkow, E. (1993) *Mol. Biol. Cell 4*, 323−335.

Walker, R. A., O'Brien, E. T., Pryer, N. K., Soboeiro, M. F., Voter, W. A., Erickson, H. P., & Salmon, E. D. (1988) *J. Cell Biol. 107*, 1437−1448.

Weingarten, M. D., Lockwood, A. H., Hwo, S. Y., & Kirschner, M. W. (1975) *Proc. Natl. Acad. Sci. U.S.A. 72*, 1858−1862.

Wiche, G., Oberkanins, C., & Himmler, A. (1991) *Int. Rev. Cytol. 124*, 217−273.

Wilson, L., Miller, H. P., Farrell, K. W., Snyder, K. B., Thompson, W. C., & Purich, D. L. (1985) *Biochemistry 24*, 5254−5262.

Wordeman, L., & Mitchison, T. J. (1994) in *Microtubules* (Hyams, J., & Lloyd, C., Eds.) pp 287−301, Wiley-Liss, New York.

Yamada, K. M., Spooner, B. B., & Wessells, N. K. (1971) *J. Cell Biol. 49*, 624−635.

Yamauchi, P. S., Flynn, G. C., Marsh, R. L., & Purich, D. L. (1993) *J. Neurochem. 60*, 817−826.

BI950655Q